Model for Airblast Atomization

N. K. Rizk* and H. C. Mongia†
General Motors Corporation, Indianapolis, Indiana 46206

The objective of fuel injection modeling activities is generally to give support to the atomizer design effort to achieve improved spray quality. In gas turbine combustors, enhanced atomization is essential for satisfactory performance because droplet sizes can have direct impact on almost all key aspects of combustion. A model that includes the integration of the submodels of airflow, fuel injection and atomization, and droplets turbulent dispersion has been formulated. The model was applied to an airblast atomizer that incorporated a short prefilming device. The predictions were validated against two-component phase Doppler interferometry data of that atomizer. The results of the present investigation demonstrate the capability of the developed model to predict satisfactorily the airflow field and spray characteristics. The results also indicate the need for detailed measurements in the near field of the atomizer in order to quantitatively verify the modeling of the initial atomization processes in this region.

Nomenclature

C_D = drag coefficient
d = droplet diameter, m
FN = atomizer flow number, m^2
g = gravitational acceleration, m/s^2
K = kinetic energy of turbulence, m^2/s^2
P = static pressure, Pa
t = film thickness, m
U = velocity of carrier phase, m/s
u = fluctuation velocity of carrier phase, m/s
V = velocity of droplets, m/s
x = axial distance, m
μ = dynamic viscosity, kg/ms
ρ = density, kg/m^3
σ = surface tension, N/m

I. Introduction

THE development of gas turbine combustors depends largely upon understanding the flow and combustion processes within the combustor. In order to accurately simulate the combustor flowfield, analytical approaches are required to account for various flow processes in addition to the details of the combustor configuration. It is equally important to establish a wide base of benchmark quality data needed for model validation. Most of the combustor performance parameters are directly related to the quality of the spray produced by the fuel injector.[1] The initial drop sizes formed at the injector exit and their trajectories coupled with the combustor primary zone aerodynamics significantly influence the evaporation and combustion characteristics of the spray.

Fuel injection calculation concepts currently in use include empirical methods that readily provide a global picture of the whole spray as well as more complex models that account for the detailed spray dynamics.[2,3] Spray correlations provide a convenient means of calculating such parameters as mean drop size and spray angle. However, it is difficult to develop a design method based only on empirical data because each correlation was derived for a certain application and may not be suitable for other types. On the other hand, analytical models have shown promising results by matching the details of the spray characteristics with reasonable accuracy. These models require either the estimation of the initial conditions of the key parameters at the atomizer exit or the utilization of measured data at some downstream distance from the atomizer as initial values.[4,5] This is due to the difficulties involved in carrying out reliable measurements in the near region of the atomizer where the initial phases of atomization occur.

It is, therefore, of great importance to establish a fundamental basis for a fuel injector design methodology that addresses the modeling of the various processes of liquid spray formation and droplet distribution within the flowfield. A model was formulated to include the numerical simulation of the airflow through and exiting from the atomizer passages, fuel filming and breakup, secondary atomization and, finally, turbulent fuel dispersion.[6] Each submodel of the overall injection model was validated in this effort separately, and the global predictions of the model were compared favorably with measurements. Recently, detailed measurements in the two-phase flowfield of an airblast atomizer were conducted and reported in Ref. 7. These data offered the opportunity to evaluate the capability of the developed model to satisfactorily predict drop size and velocity distributions in the flowfield. The results of this study are given in the following sections.

II. Experimental

The atomizer used for the present investigation is illustrated in Fig. 1. It is a pure airblast atomizer where the fuel is injected through six tangential ports in a swirl chamber to form a sheet that is immediately exposed to air on both sides. The outer air flows through a swirler, while the inner air passes through a number of tangential slots to the central passage. The total airflow-effective area of the atomizer was found to be about 19.5 mm^2. The atomizer is designed for use in small gas turbine engines.

The details of the experiment and test facilities are included in Ref. 7. A brief description of test conditions and method of measurements is given in the following paragraphs. The selected air-to-fuel ratio was 1.0 with a fuel flow rate of 0.0021 kg/s that corresponded to the engine cruise operating mode. The atomizer sprayed methanol downward into a square duct and was mounted on a traverse system that provided three degrees of translational freedom. A screen air-bulk velocity of 1 m/s was provided to avoid the recirculation of the fine droplets to the measurement control volume.

Two-component phase Doppler interferometry was used for the simultaneous measurement of droplet size and veloc-

Presented as Paper 89-2321 at the AIAA/ASME/SAE 25th Joint Propulsion Conference, Monterey, CA, July 10–12, 1989; received Sept. 28, 1989; revision received Dec. 27, 1989.

*Staff Research Scientist, Combustion Department, Allison Gas Turbine Division. Member AIAA.

†Chief, Combustors Research and Development, Combustion Department, Allison Gas Turbine Division. Member AIAA.

ity.[8] The velocity of the gas phase was measured by seeding the airflow with alumina oxide particles of nominal size of 1 μ. In two-phase flow, the gas velocity within the spray was deduced by measuring the velocity of the particles which was small enough to track the flow.

III. Fuel Injection Design System

The overall fuel injection concept involves the integration of three main submodels of airflow, fuel injection and atomization, and droplet turbulent dispersion. The characteristics of air flowfield are needed to evaluate various filming and atomization processes, and the two-phase flow model is used to predict the spray dispersion within the field. In the following subsections, the details of the model components are described in addition to the model application to the atomizer shown in Fig. 1.

A. Airflow Modeling

In order to establish the air flowfield within and downstream of the atomizer, a boundary-fitted, curvilinear grid system is used because the fuel nozzle geometry is too complex to be accurately represented by a cylindrical coordinate system.[9] The present calculation was obtained using a 49 × 45 grid network, as shown in Fig. 2.

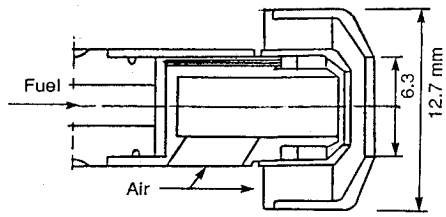

Fig. 1 Airblast atomizer used in the study.

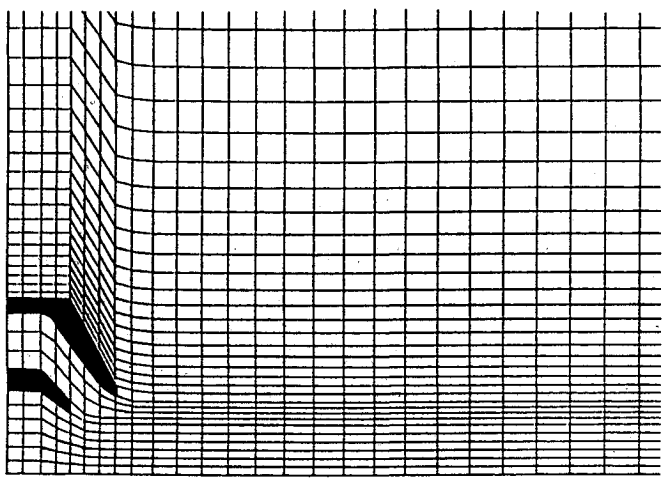

Fig. 2 Grid arrangement used for computations.

The elliptic two-dimensional transport equations of continuity, momentum, and the standard $k-\varepsilon$ turbulence model for an incompressible flow, using Cartesian tensor notation, are given by

$$\frac{\partial U_i}{\partial x_i} = 0 \tag{1}$$

$$\frac{\partial}{\partial x_j}(\rho U_j U_i) = -\frac{\partial P}{\partial x_i} + \frac{\partial}{\partial x_j}\left(\mu \frac{\partial U_i}{\partial x_j} - \overline{\rho u_i u_j}\right) \tag{2}$$

where $U_i + u_i$ is the local instantaneous velocity component in the i direction, and $-\rho\overline{u_i u_j}$ are the Reynolds stresses. The transport equations for the turbulent kinetic energy K and its dissipation rate ε are given by

$$\frac{\partial}{\partial x_j}(U_j \rho K) = \frac{\partial}{\partial x_j}\left(\frac{\mu_{\text{eff}}}{\sigma_k}\frac{\partial K}{\partial x_j}\right) + G_k - \rho\varepsilon \tag{3}$$

$$\frac{\partial}{\partial x_j}(U_j \rho \varepsilon) = \frac{\partial}{\partial x_j}\left(\frac{\mu_{\text{eff}}}{\sigma_\varepsilon}\frac{\partial \varepsilon}{\partial x_j}\right) + C_{\varepsilon 1}\frac{\varepsilon}{K}G_k - C_{\varepsilon 2}\rho\frac{\varepsilon^2}{K} \tag{4}$$

where σ_k and σ_ε are the equivalent turbulent Prandtl numbers for K and ε, G_k is the local production of turbulent kinetic energy, and μ_{eff} is the summation of the dynamic viscosity and eddy viscosity of the gas phase. The coefficients $C_{\varepsilon 1}$ and $C_{\varepsilon 2}$ are in the turbulence model.

The discretization of the equations is performed in a generalized coordinate system. The momentum equations are written in terms of covariant velocity components. Because of the spatial variation of the base vectors associated with these velocity components, curvature source terms appear in the governing equations.[10]

The presence of the spray droplets within the gas phase is accounted for by the inclusion of the appropriate source terms that consider the effects of droplet mass and the interphase friction.

The predictions of the airflow model are compared with the measurements at three axial locations of 50, 75, and 100 mm from the nozzle exit in Figs. 3 and 4 for axial and tangential velocity components, respectively. It is seen that the calculations are in good agreement with the axial velocity data at the three measurement locations. The trends of variation of the tangential component with the radial position are similar in both the model predictions and data. However, the calculated values are at higher levels. These results indicate that the $k-\varepsilon$ turbulence model is fairly accurate in providing the axial velocity profiles of the atomizer air. The model has less

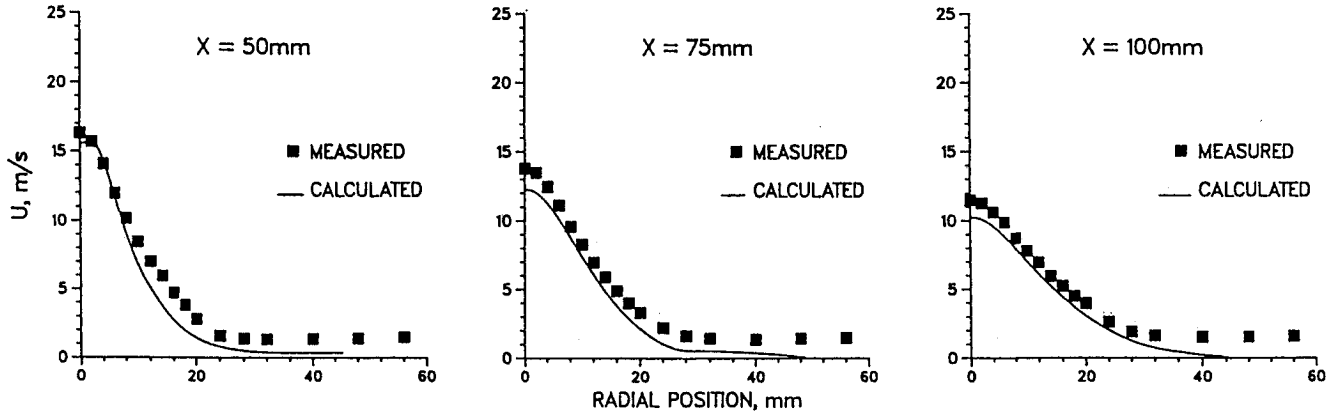

Fig. 3 Comparison of calculated axial velocity with measurements.

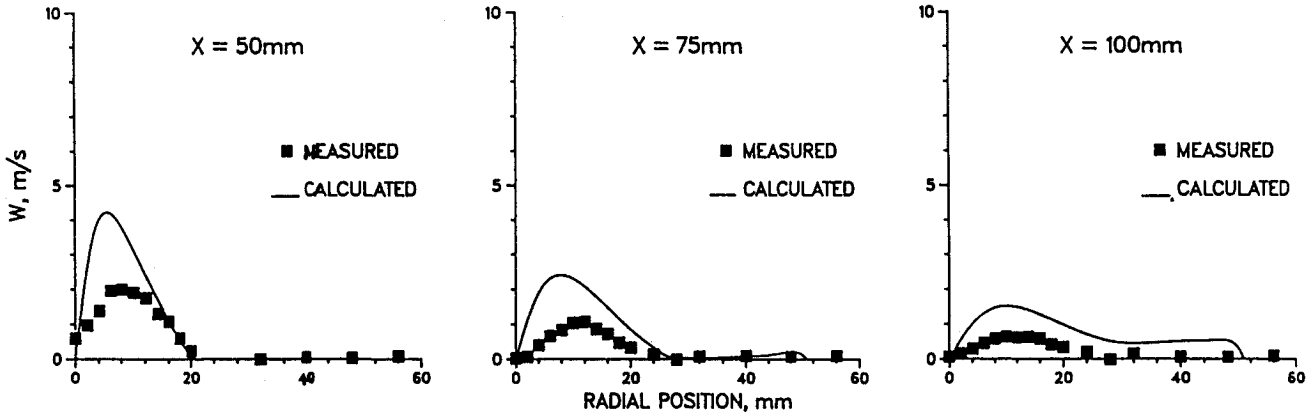

Fig. 4 Comparison of tangential velocity calculation and measurement.

success in predicting the swirl component of the flow. The use of other schemes, such as an algebraic stress model may enhance the prediction of the flow when significant swirl exists.

B. Fuel Injection and Atomization Model

The fundamental processes of the fuel atomization include liquid formation into sheet, its subsequent disintegration into ligaments and drops, and in-flight breakup that the drops may undergo due to the relative air velocity. The formation of liquid film in the airblast atomizer may be achieved by spreading the liquid onto a prefilmer under the effect of high velocity air. The prefilmer geometry, fuel and air properties, and operating parameters are the main factors controlling the film thickness. The model adopted to determine liquid film thickness is based on the evaluation of the interfacial friction factor between the airstream and liquid film within the atomizer.[11]

The film thickness t is given by

$$t^2(1 + 300\, t/d_h) = 16.1\mu_L W_L R_e^{0.25}/\rho_L \rho_a d_0 U_a^2 \tag{5}$$

In this equation, d_0 is prefilmer diameter, d_h is hydraulic diameter of air passage, W_L is liquid flow rate, U_a is air velocity given by the carrier phase model, and R_e is Reynolds number of airflow. The airflow over the film smooths out the film on the prefilmer and guides its discharge from the atomizer.

In some other designs, the filming surface is made so short that the actual film leaving the atomizer is controlled by the swirl chamber and atomizer lip geometry. The flowing air has no effect on the film thickness in this case, and the mechanism of film formation is more or less similar to the one associated with pressure swirl atomization.[12] The film thickness in this case is given by

$$t = 3.66\left[\frac{\mathrm{FN}\mu_L d_c}{(\rho_L\, \Delta P_L)^{0.5}}\right]^{0.25} \tag{6}$$

FN is the atomizer flow number, d_c the characteristic dimension of fuel passage, and ΔP_L the fuel pressure drop. The film discharges at an angle θ given by

$$\cos^2\theta = \frac{1 - A_c}{1 + A_c} \tag{7}$$

A_c is the area ratio of air core to fuel passage.

The breakup of the liquid sheet into ligaments and drops involves the instability of the liquid stream and its tendency to form waves as the result of the interaction with the air. Being unstable, the wave amplitude rapidly increases to a critical value at which the liquid disintegrates into ligaments, which in turn break up into drops. Reference 13 shows that, with an increase in air velocity, the liquid sheet disintegrates earlier so that ligaments are formed nearer the lip. These ligaments tend to be thinner and shorter and disintegrate into smaller drops.

The balance of forces caused by gas pressure, surface tension, liquid inertia, and viscosity controls the breakup mechanism of the sheet.[14] The governing equation can be written as follows:

$$2\rho_a n U_r^2 - 2\sigma n^2 - \rho_L t\left(\frac{\partial f}{\partial T}\right)^2 - \mu_L t n^2\left(\frac{\partial f}{\partial T}\right) = 0 \tag{8}$$

where U_r is the relative velocity, f the total growth of wave, T the time, and n the wave number of the disturbance imposed on the liquid stream of thickness t and is given by

$$n = \frac{F^2 \rho_a U_r^2}{2\sigma} \tag{9}$$

and F is the ratio of wave growth of liquid to that of inviscid liquid. The maximum value of F is given by

$$1 - F^2 - VF^3 = 0 \tag{10}$$

where

$$V = \frac{\mu_L \rho_a U_r^2}{2}\left(\frac{t}{2\rho_L \sigma^3}\right)^{0.5} \tag{11}$$

It is shown in Ref. 14 that the breakup of liquid sheets due to the wave growth concept occurs as the total growth of the wave f, which is given by the natural logarithm of the ratio of wave amplitude to amplitude of initial disturbance, approaches a constant value of 12. The high speed photography of the breakup of the liquid sheet at the atomizing edge of the fuel injector indicates that the ligaments are drawn from the sheet at the atomizer lip or at a small downstream distance as the atomizing air velocity decreases.[2,13] The photographs show that the free ends of the ligaments disintegrate, and the detached parts rapidly contract to spherical drops under the effect of surface tension.

Because the forces caused by the high relative motion between the air and the formed ligaments correspond to those used to derive the above equations, the procedure adopted in the present model uses the same outline of the preceding mechanism. The time taken to reach the total wave growth at breakup is evaluated using an average value of the total relative velocity and ligament dimension through an iterative procedure. An appropriate dimension to use in the calculation of the ligament acceleration, due to air effect, and its breakup is the diameter. The average length of the ligament is then determined from the breakup time and the average ligament velocity.

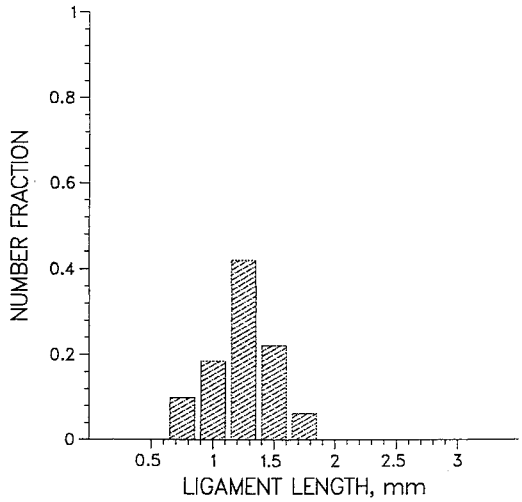

Fig. 5 Calculated ligament length distribution.

The disintegrated parts of the ligaments instantly form spherical drops in the calculation corresponding to a full wave length, the average size of which is estimated from the conservation of mass of each part. The drops continue to move in the domain at the velocity of ligament at the breakup point. Several modes of secondary breakup of the drops because of their relative velocity with the surrounding air have been identified in the literature. Notable examples are the formation of a central membrane in the drop and its subsequent bursting as a bag as well as the detachment of layers off the drop. The layers break up into drops, the diameter of which may be the same order of magnitude of the length of the disturbing wave or the thickness of the boundary layer generated on the drop.[15,16,17]

The application of such approaches to simulate actual sprays has shown that the former mode, which is governed by a critical Weber number concept, rarely occurs. The latter mechanism yields unrealistic drop-size distributions that contain a much larger proportion of fine drops than those observed in real sprays. The calculation approach that is found to give reasonable predictions of the spray drop sizes is described in the following paragraphs.

The drops formed at breakup are allowed to deform under the effect of high-velocity air, according to the Weber number level experienced by the drop. The deformation of the drops is modeled considering a change of sphericity of drops with time toward circular disk shapes. The deformed drops may undergo secondary atomization, which is modeled using the stripping breakup concept.[16] This is governed by a critical Reynolds number that is based on the relative velocity U_r and instantaneous drop size R. The rate of change of drop size is given by

$$\frac{dR}{dt} = -A\left(\frac{\rho_a}{\rho_L}\right)^{0.33}\left(\frac{\mu_L\rho_a}{\mu_a\rho_L}\right)^{0.167}\left(\frac{\mu_L U_r}{\rho_L R}\right)^{0.5} \tag{12}$$

The variable A is a constant of the order of unity, and μ and ρ are viscosity and density of liquid and air that are defined by the subscripts L and a, respectively. As the drop size changes, the drop number is changed accordingly in each drop parcel. This procedure is followed because of the lack of details on the sizes of the droplets formed from the parent drop and to avoid impractically long involved calculations if such a distribution is assumed at drop breakup.

The concept of the breakup of a liquid film of a uniform thickness into ligaments and drops leads to the formation of a single-size drop spray. Actual gas turbine atomizer spray, however, contains droplets that vary over a wide range of sizes. This is mainly because of the nonuniformity in the ligament formation and breakup resulting from the turbulent nature of the atomizing air and the local variation in film thickness. Initially, these factors were accounted for by adopting an empirical approach that used the spray Sauter mean diameter SMD, given by the model, to describe the whole drop size distribution at the completion of the atomization process.[18] Through an iterative procedure, the initial drop size distribution at ligaments breakup was determined and tracked through the atomizer flowfield.[6] The model gave a good agreement with the overall spray SMD measurement.

In order to extend the capability of the model, in the present effort, to predict the details of the atomizer flow domain, the liquid film thickness at breakup is considered to vary around the mean value, with a probability distribution following a Gaussian curve. To account for the effects of the turbulent airstreams on ligament formation and breakup, similar approaches are followed to define the distributions of the ligament exit angle and disintegrated length around the nominal values. The resulting ligament length distribution is given in Fig. 5. Although detailed measurements in this critical region are needed to verify the results, the range of ligament length observed in the figure is in reasonable agreement with the data reported in Ref. 13. The large number of droplets formed by this manner is tracked throughout the flowfield using the two-phase flow model, described in the following subsection, and considering the secondary atomization effects. The initial conditions include drop size distribution, number density, and velocity components of each formed droplet.

C. Two-Phase Flow Model

Detailed knowledge of the spray dynamics is fundamental to the evaluation of the spray trajectories and evaporation. The two-phase flow model considers the effects of the instantaneous gas droplet relative velocity on the transfer quantities and the interaction of the mean and fluctuating motion between the two phases.[5] The model consists of a fully coupled combination of Lagrangian droplet and Eulerian fluid calculations.

The equation of motion of each computation droplet in the ith direction is given by

$$\frac{dV^k}{dt} = \frac{U_i - V_i^k}{\tau_d^k} + g_i \tag{13}$$

where

$$\tau_d^k = \frac{4d^k\rho_L}{3C_D^k\rho_a|U - V^k|} \tag{14}$$

Drag coefficient C_D is calculated from the standard experimental drag curve of solid sphere, d^k and V^k are instantaneous diameter and velocity of droplet k, and ρ_a and ρ_L are carrier phase and droplet densities. U_i is the summation of the mean velocity of the carrier phase and the fluctuating velocity u_i that is chosen randomly from an isotropic Gaussian distribution with mean square deviation of 2/3 of the turbulent

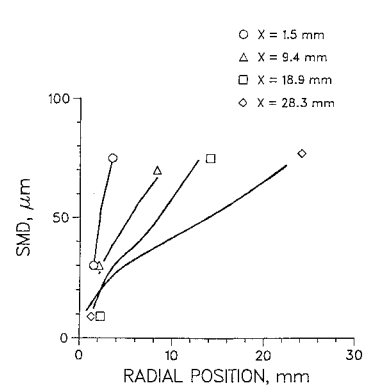

Fig. 6 Calculated radial drop size distribution near atomizer.

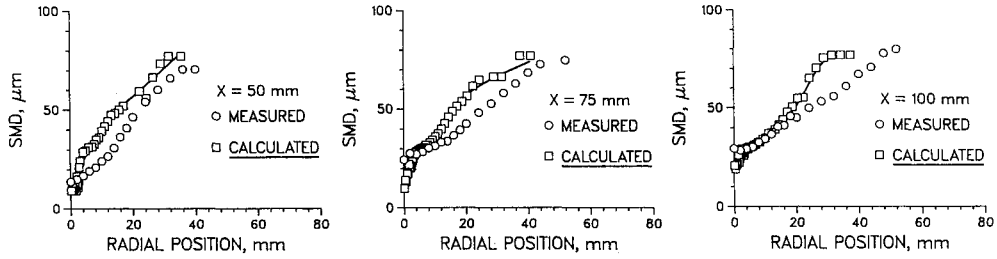

Fig. 7 Comparison of radial distribution of SMD with measurement.

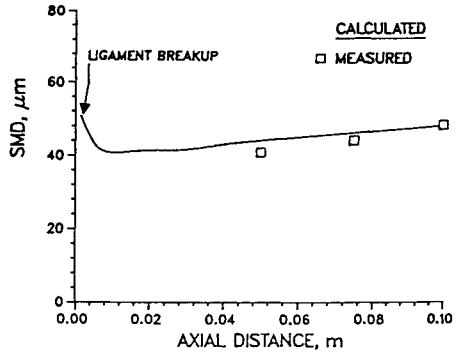

Fig. 8 Axial distribution of SMD.

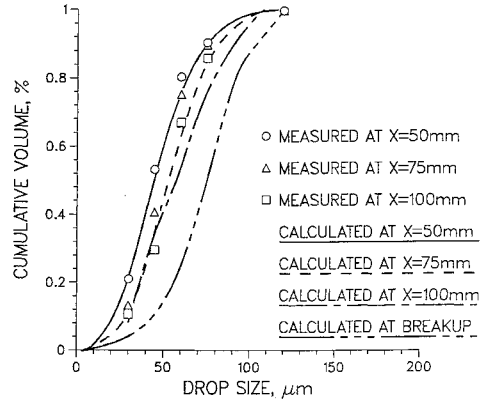

Fig. 9 Drop-size distribution in spray.

kinetic energy of the gas phase. The droplet location at any instant of time is given by

$$\frac{dx_i^k}{dt} = V_i^k \tag{15}$$

For each droplet, after a turbulent correlation time τ, a new value for u_i is chosen. The τ is the minimum of the two scales: one is a typical turbulent eddy lifetime, and the other is the residence time of the droplet in the eddy. If a sufficiently large number of droplets are tracked this way, the averaged behavior should yield the effects of the turbulence of the air flowfield on the spray dispersion. The source terms because of the spray presence in the flowfield are used to update the gas flow calculations by introducing the following term in the carrier phase momentum equation:

$$-\sum_k \phi \frac{3\rho_L}{4d^k} C_D^k |U - V^k| \tag{16}$$

where ϕ is the droplet volume fraction in the control volume. Because approximately 800 drops are considered in the calculations to form at ligament breakup, each drop is tracked between 10 to 20 times through the turbulent flowfield to render the approach practical.

IV. Results and Discussion

In this section, the spray characteristics and dispersion in the flowfield, as given by the model, are presented and compared with the experimental data whenever applicable. Figure 6 illustrates the variation in the SMD radial distribution as the droplets formed at ligament breakup move downstream of the atomizer. It is noticed that smaller droplets start to appear further downstream in addition to a significant increase in the radial spread of droplets. The calculated radial distribution of SMD at axial distances of 50, 75, and 100 mm is compared with the measured data in Fig. 7. Good agreement is observed in the figure; although it appears that the radial spread of droplets is somewhat less than the measured one. This is attributed to the narrower air velocity profiles calculated for the atomizer as compared with the data in Fig. 3.

The variation of the overall SMD at each axial location with the downstream distance is illustrated in Fig. 8. The figure indicates an initial decrease in SMD as a result of the breakup of large drops, which is followed by a steady increase in SMD with distance. This is caused by the continuous changes in the relative velocity between various drop-size groups that control the number density of each size at each axial location. Because no droplet evaporation or coalescence is considered in the present approach, the changes in drop size at larger downstream distances could be avoided by considering the velocity of each drop-size parcel in the calculation of the overall SMD at each location. The calculated drop-size distribution at the three axial distances and at the ligament breakup are plotted in Fig. 9 along with the measured ones. Good agreement between the measurements and the predictions is illustrated in the figure. It is also seen that the whole distribution moves toward a smaller size range as the spray travels away from the nozzle; then the trend is reversed at larger distances.

The average axial velocity of all droplets as given by the model is plotted in Fig. 10 against the radial position at the three measurement planes of 50, 75, and 100 mm. The figure illustrates the capability of the model to follow the data trends. The measurements, however, show higher velocities toward the edge of the spray. This is the result of the discrepancies between the predicted and measured air velocity near the edge of the spray. While the measured data show that the air velocity profile extends to larger radii, the droplet velocity diminishes at a smaller distance from the centerline. The predicted profile peaks slightly off the spray centerline, especially at axial stations close to the atomizer. At these locations, it has been seen that higher tangential velocity of air is predicted with a slightly lower axial component at centerline. Moreover, the initial direction of drop trajectory at the atomizer exit expands outward. All of these factors tend to shift the drops away from the atomizer centerline.

The fuel injection model also provides the velocity of each drop size group at various locations of the spray. The axial velocity profiles of the smallest and largest size groups considered in the investigation are given in Fig. 11. The measured

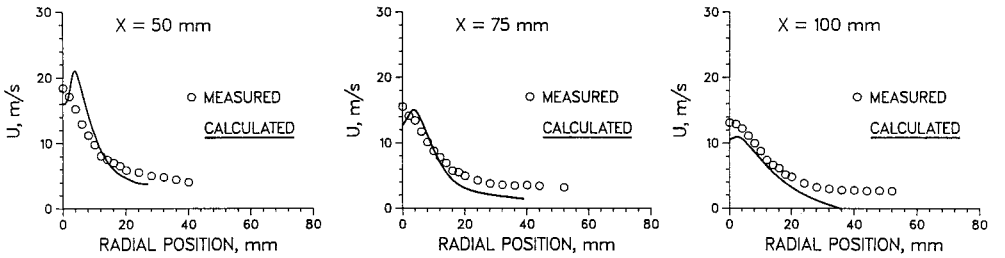

Fig. 10 Average droplet axial velocity.

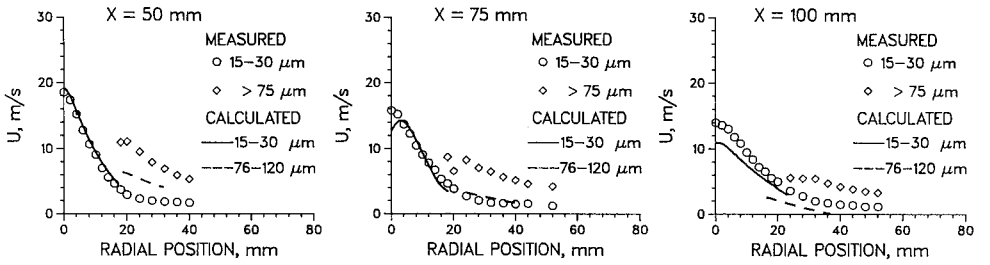

Fig. 11 Axial velocity profile for different drop-size groups.

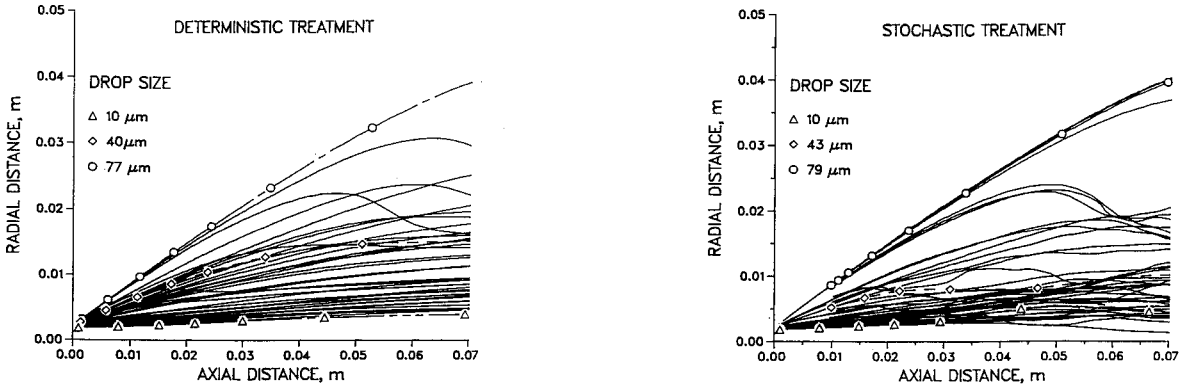

Fig. 12 Calculated droplet trajectories.

profiles of the two extreme groups are also plotted in the figure. The velocities of the other size groups fall somewhere in between the two profiles. It is observed that the model is fairly accurate in predicting the velocity of the 15–30 μ size group. The figure also shows that the predicted profiles for the largest drops, which exist toward the outer region of the spray, are much lower in values than the measured velocities of this group size. This is attributed, once again, to the under-prediction of the carrier-phase velocities at large radial locations.

The predictions of drop trajectory in the flowfield for all the drops formed at ligament breakup were performed under no turbulent flow conditions (deterministic treatment) and with the effects of turbulence (stochastic model). A number of drop trajectories were selected for each case to represent various drop sizes in spray, and these trajectories are plotted in Fig. 12. The drop sizes quoted in this figure are the sizes at the completion of the atomization process. The figure shows the smooth trajectories of the deterministic treatment and the turbulent dispersion of the smaller drops when the limited stochastic treatment is adopted. It is also noticed that the larger drops are able to penetrate the air flow streamlines more than the smaller drops, and they are less affected by the turbulent behavior of the carrier phase.

V. Conclusion

In order to optimize the design of gas turbine combustor components, accurate analytical tools are highly required to guide the design and development of the combustor. Modeling of the fuel injector is therefore needed as an important part of the design system.

An atomization model has been formulated and validated against data of detailed measurements in the flowfield of a small airblast atomizer. The model combines airflow calculations, fuel preparation and breakup into spray, and the dispersion of the droplets in the atomizer flow domain. It is concluded that

1) Satisfactory agreement between data and predictions of the axial air velocity profiles is observed. However, the tangential velocity component is overpredicted in most cases.

2) Ligament formation and breakup modeling results agree qualitatively with the data reported in the literature, which emphasizes the need for accurate measurements in the near region of the atomizer.

3) The model, with a reasonable degree of success, predicts the radial distribution of drop sizes in the spray at three axial locations of 50, 75, and 100 mm from the atomizer. Verification of the model at smaller distances requires additional measurements for this atomizer.

4) In general, the calculated axial velocity profiles of the drops follow the experimental ones, with the best fit occurring for the small drops. The velocity of larger drops are underpredicted.

5) The effect of the inclusion of the carrier phase turbulence in the calculation is to increase the diffusion of the smaller drops in the spray with little or no effect on the larger

drops. It also helps in bringing the fine droplets closer to the spray centerline.

Acknowledgments

The authors would like to thank G. S. Samuelsen, V. G. McDonell, and the staff of the University of California Combustion Laboratory, Irvine, California for providing the results of the spray measurements that were used for model validation.

References

[1]Lefebvre, A. H., "Fuel effects on Gas Turbine Combustion-Ignition, Stability, and Combustion Efficiency," *Transactions of ASME, Journal of Engineering for Gas Turbine and Power*, Vol. 107, Jan. 1985, pp. 24–37.

[2]Lefebvre, A. H., "Atomization and Spray," Hemisphere, Washington DC, 1989, pp. 201–272.

[3]Reitz, R. D., and Bracco, F. V., "Mechanism of Atomization of a Liquid Jet," *Physics of Fluids*, Vol. 25, No. 10, 1982, pp. 1730–1742.

[4]Sturgess, S. A., Syed, S. A., and McManus, K. R., "Calculation of a Hollow-Cone Spray in a Uniform Air Stream," *Journal of Propulsion and Power*, Vol. 1, No. 5, 1984, pp. 360–368.

[5]Mostafa, A. A., and Mongia, H. C., "On the Modeling of Turbulent Evaporating Sprays: Eulerian Versus Lagrangian Approach," *International Journal of Heat Mass Transfer*, Vol. 30, No. 12, 1987, pp. 2583–2593.

[6]Rizk, N. K., Mostafa, A. A., and Mongia, H. C., "Modeling of Gas Turbine Fuel Nozzles," *Atomization and Spray Technology*, Vol. 3, No. 4, 1987, pp. 241–260.

[7]McDonell, V. G., and Samuelsen, G. S., "Evolution of the Two-Phase Flow in the Near Field of an Air-Blast Atomizer Under Reacting and Non-Reacting Conditions," *Fourth International Symposium on Applications of Laser Anemometry to Fluid Mechanics*, Lisbon, Portugal, July 1988.

[8]Bachalo, W. D., and Houser, M. J., "Phase/Doppler Spray Analyzer for Simultaneous Measurements of Drop Size and Velocity Distributions," *Optical Engineering*, Vol. 23, No. 5, 1984, pp. 583–590.

[9]Patankar, S. V., "Numerical Heat Transfer and Fluid Flow," McGraw-Hill, New York, 1980, pp. 11–20, 79–137.

[10]Karki, K. C., and Patankar, S. V., "Calculation Procedure for Viscous Incompressible Flows in Complex Geometries," *Numerical Heat Transfer*, Vol. 14, 1988, pp. 295–307.

[11]Rizk, N. K., and Lefebvre, A. H., "Influence of Liquid Film Thickness on Airblast Atomization," *Journal of Engineering Power*, Vol. 102, 1980, pp. 706–710.

[12]Rizk, N. K., and Lefebvre, A. H., "Internal Flow Characteristics of Simplex Swirl Atomizers," *Journal of Propulsion and Power*, Vol. 1, No. 3, 1985, pp. 193–199.

[13]Rizk, N. K., "Studies on Liquid Sheet Disintegration in Airblast Atomizers," Ph.D. Dissertation, Cranfield Inst. of Technology, Bedford, England, UK, 1977.

[14]Dombrowski, N., and Johns, W. R., "The Aerodynamic Instability and Disintegration of Viscous Liquid Sheets," *Chemical Engineering Science*, Vol. 18, 1963, pp. 203–214.

[15]Giffen, E., and Muraszew, A., *The Atomization of Liquid Fuels*, Chapman & Hall Ltd., London, 1953.

[16]Jenkins, D. C., and Booker, J. D., "The Time Required for High Speed Air Streams to Disintegrate Water Drops," Ministry of Aviation, Aeronautical Research Council, London, CP 827, 1965.

[17]Reitz, R. D., and Diwakar, R., "Effect of Drop Breakup on Fuel Sprays," *Society of Automotive Engineers*, Warrendale, PA, SAE Paper 860469, 1986.

[18]Custer, J. R., and Rizk, N. K., "Influence of Design Concept and Liquid Properties on Fuel Injector Performance," *Journal of Propulsion and Power*, Vol. 4, No. 4, 1988, pp. 378–384.